CONCRETE RESEARCH LETTERS

www.crl.issres.net

Vol. 2 (3) – Sep. 2011

Corrosion Damage in Reinforced Concrete identified by AE

Yuma Kawasaki[c], Misuzu Kitaura, Tomoe Kobarai and Masayasu Ohtsu[1]

[1] *New Frontier Sciences, Graduate of Science and Technology*
Kumamoto University, JAPAN

[2] *Department of Civil and Environmental Engineering, Graduate of Science and Technology*
Kumamoto University, JAPAN

Abstract

Deterioration and damage in reinforced concrete (RC) have been reported world-wide. One of critical causes is a salt attack. Thus, monitoring against corrosion damage is a key issue. To identify the onset of corrosion and the nucleation of corrosion-induced cracks due to expansion of corrosion products, continuous acoustic emission (AE) monitoring is available. SiGMA (Simplified Green's functions for Moment tensor Analysis) procedure is applied to AE waveforms to identify source kinematics of micro-cracks in the corrosion process. Results show that the onset of corrosion and the nucleation of corrosion-induced cracks in RC are visually located. Further, corrosion damage due to the expansion of corrosion products is quantitatively identified.

Keywords: Acoustic emission; Corrosion-induced cracks; Reinforced concrete; Salt attack; SiGMA

1. Introduction

In concrete engineering, it is seriously known that concrete structures are no longer maintenance-free. In this respect, non-destructive evaluation (NDE) of corrosion damage was investigated [1]. In reinforced concrete (RC) structures, passive films on the surface of rebars (reinforcing steel-bars) could be broken due to attack of chloride ions, and activated ferrite ions lead to the corrosion of rebars. Since almost of all concrete structures are reinforced by rebars, the corrosion due to salt attack has been referred to as the most critical deterioration of RC structures. So far, electrochemical techniques of the half-cell potentials and the polarization resistance are widely employed to evaluate corrosion of rebar. Recently, acoustic emission (AE) method has been introduced to successfully detect corrosion-induced cracks in concrete [2].

According to a phenomenological model of rebar corrosion in seawater environments, it is reported [3] that a typical corrosion loss during the corrosion process can be divided into four phases shown in Fig. 1. At Phase 1, the onset of corrosion is initiated. The corrosion process is

[c] Corresponding Author: Yuma Kawasaki
Email: 101d9107@st.kumamoto-u.ac.jp Telephone: +81 963423606 Fax: +81 963423507

activated by the rate of penetration of oxygen and water. Then a corrosion loss decreases at Phase 2, because the flow of oxygen is eventually inhibited by corrosion products at the surface of rebar. Thus, the increase in the corrosion loss is saturated during Phase 2. As the corrosion process advances, the corrosion loss again increases during Phases 3 and 4, where the corrosive zone penetrates into rebar and the expansion of corrosion products occurs. Eventually corrosion-induced cracks of concrete are nucleated.

Based on this model, continuous AE measurement was conducted in a cyclic wet and dry test. In order to clarify kinematical information of internal cracks at these phases, AE events are detected. Thus, kinematics of cracks are studied by applying SiGMA (Simplified Green's functions for Moment tensor Analysis) analysis.

2. AE Analysis

AE events are associated with cracking and are detected by AE sensors as electrical signals, which are amplified, filtered, and processed. An AE signal is characterized by employing AE parameters such as energy, counts, event, amplitude, rise time and duration as illustrated in Fig. 2. By employing a multi-channel system, SiGMA analysis consists of 3-D (three-dimensional) AE source location procedure and the moment tensor analysis for AE source. Two parameters of the arrival time (P1) and the amplitude of the first motion (P2) are read from a waveform and applied to the analysis. In the location procedure, AE source ***x'*** is located from the arrival time difference t_i between the observation point x_i and x_{i+1}, by solving equations,

$$R_i - R_{i+1} = |x_i - x'| - |x_{i+1} - x'| = v_p t_i \quad (1)$$

Here, v_p is the velocity of P-wave and R_i represents the distance between AE source and observation point x_i. After solving Eq. 1 and locating AE source, the amplitudes of the first motion (P2) are substituted into the following equation.

$$A(x) = C_S \cdot \frac{\mathrm{Ref}(t,g)}{R} \cdot g_p g_q M_{pq} \cdot DA \quad (2)$$

Here, $A(x)$ is the amplitude of the first motion of P-wave and Cs is the calibration coefficient of the sensor sensitivity and material constants. The reflection coefficient $\mathrm{Ref}(t,g)$ is obtained as t is the direction of sensor sensitivity. DA is area of crack surface, and M_{pq} is the moment tensor. g is the

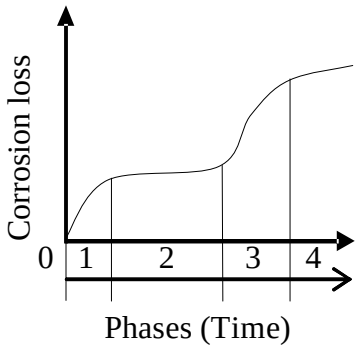

Figure 1. Typical corrosion loss for steel in seawater immersion

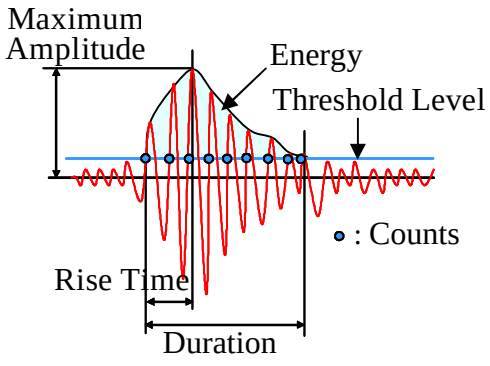

Figure 2. AE waveform parameters

direction vector of distance R from the source to the observation point ***x***. Since the moment tensor M_{pq} is symmetric and of the second order, the number of independent unknown components of M_{pq} is six. Thus, to determine the moment tensor components, waveforms are to be detected at more than six sensors. The classification of a crack is performed by the eigen-value analysis of the moment tensor [4]. Eventually, micro-cracks are classified and visualized by employing the Light Wave 3D software as shown in Fig. 3. Here, an arrow vector indicates the direction of a crack motion vector, and a circular plate indicates the orientation of a crack surface, which is perpendicular to a crack normal vector.

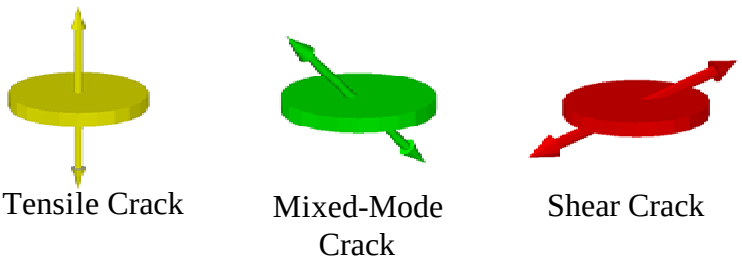

Figure 3. 3-D Models displayed for tensile, mixed-mode and shear cracks

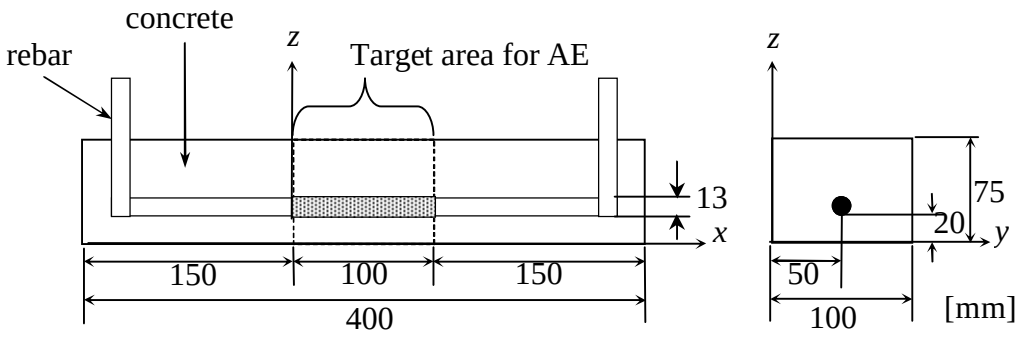

Figure 4. Sketch of reinforced concrete beam tested.

3. Experimental set-up

RC specimens of dimensions 75 mm× 100 mm × 400 mm were made. Configuration of the specimen is illustrated in Fig. 4. A rebar of 13 mm diameter was embedded with 20 mm cover-thickness for longitudinal arrangement. Mixture proportion of concrete is given in Table 1. Here, NaCl solution is employed as mixed-water. Following the standard curing for 28 days, corrosion process under salt attack was simulated by cyclic wet and dry condition.

TABLE 1. MIXTURE PROPORTION OF CONCRETE

Maximum gravel size (mm)	Water to cement ratio W/C (%)	Weight per 1m^3 concrete					Slump (cm)	Air (%)
		Water (kg)	Cement (kg)	Sand (kg)	Gravel (kg)	NaCl (kg)		
10	55	185	336	823	1019	0.210	8	5

In the cyclic wet and dry test, specimens were cyclically put into the container filled with 3% NaCl solution for a week and subsequently taken out of the container to dry under ambient temperature for another week. AE measurement was continuously conducted, by using AE measurement system (DiSP). Six AE sensors of 150 kHz resonance were attached to the surface of the specimen as shown in Fig. 5. The frequency range of the measurement was 10 kHz to 2 MHz and total amplification was 60 dB gain. For event counting, the dead-time was set to 2 msec and the threshold level was set to 40 dB gain.

4. Results and discussion

Cumulative AE hits and AE events for every 1 hour of 6 channels are shown in Fig. 6. Each AE event was detected by all 6 AE sensors. AE hits and AE events start to gradually increase during the first 28 days. Then, AE hits have sharply increased at 28 days elapsed. From 42 days elapsed to 182 days, AE hits and AE events keep increasing consectively. The curve of cumulative AE hits is in remarkable agreement with the curve of corrosion loss in Fig. 1. This leads to the fact that the onset of corrosion started during the first 42 days and the expansion of corrosion products

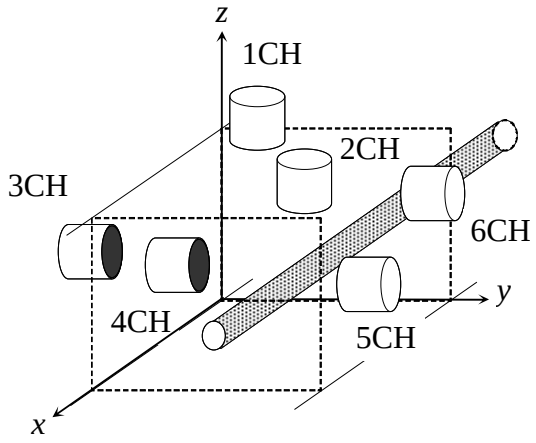

Figure 5. Set of AE sensors

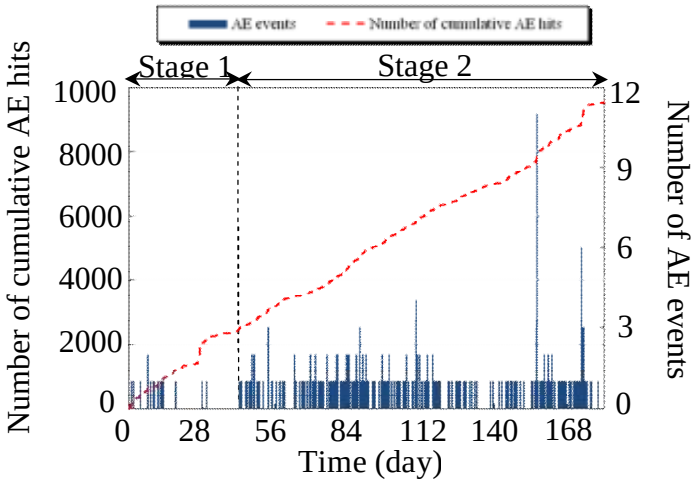

Figure 6. Number of cumulative AE hits and AE events

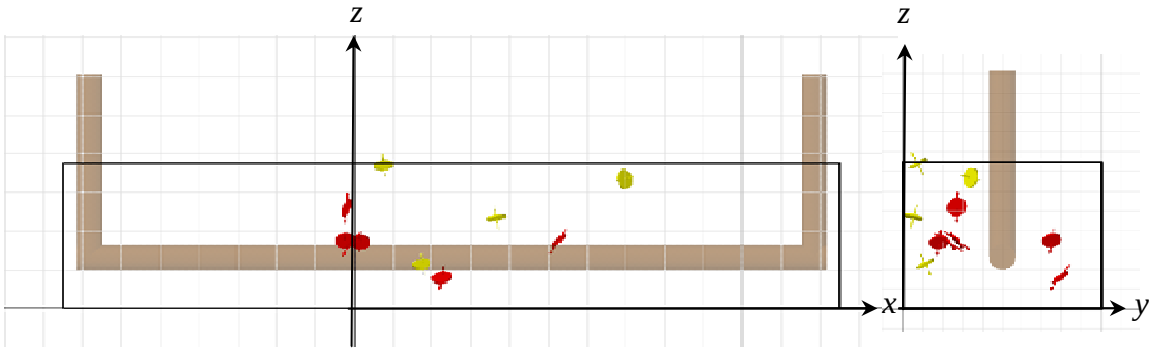

Figure 7. Results of SiGMA analysis during the first 42 days (Stage 1)

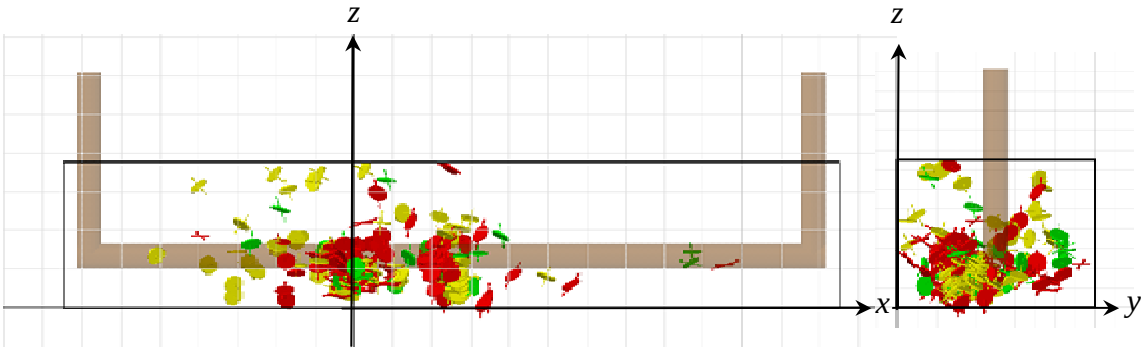

Figure 8. Results of SiGMA analysis from 42 days to 182 days (Stage 2)

occurred from 42 days to 63 days. Accordingly AE events observed from 63 days to 182 days could result from corrosion-induced cracking in concrete.

In the SiGMA analysis, AE event definition time (EDT) is set to 100μsec. EDT is applied to recognize AE waves occurring within the specified time from the first-hit and to classify them as part of the current event. Results of the SiGMA analysis during the first 42 days are illustrated in Fig. 7. During the period, only 10 AE events are determined. These events are located mostly surrounding the rebar. Results of the SiGMA analysis from 42 days to 182 days are illustrated in Fig. 8. 159 AE events are determined. Many of AE events are observed around the rebar. At 126 days, surface cracks were visually found. AE cluster of the total was compared with the surface crack observed at the bottom of the specimen. Then, it is demonstrated that locations and orientations of AE sources are in remarkable agreement with the surface cracks observed. This suggests that generation of the corrosion-induced cracks in concrete could be visualized by conducting the SiGMA analysis continuously.

5. Conclusion

In the cyclic wet and dry test, the onset of corrosion and the nucleation of corrosion-induced cracking in concrete are reasonably distinguished from AE activity. This confirms that these two stages can be identified by AE monitoring.

AE activity is low at the onset of corrosion. Thus, the number of AE events located is a few. Then, AE sources clearly observed at the nucleation of cracking, as the cracks occurred around the rebar. Results of the SiGMA analysis during the corrosion process are in remarkable agreement with locations of the surface cracks. Results show that corrosion-induced cracks can be identified by the SiGMA analysis of AE monitoring.

References

[1] Dubravka, B., Dunja, M. and Dalibor, S. *Non-Destructive Corrosion Rate Monitoring for Reinforced Concrete Structures*, 2000, *15th WCNDT*.

[2] Ohtsu, M. *Detection and Identification of Concrete Cracking in Reinforced Concrete by AE*, Review of Progress in Quantitative NDE. 2003, *AIP conference 2003*, Proc. **657**(22B): pp. 1455-1462.

[3] Melchers, R. E. and Li, C. Q. *Phenomenological Modeling of Reinforcement Corrosion in Marine Environments*, ACI Materials Journal, 2006, **103**(1): pp. 25-32.

[4] Ohtsu, M. *Simplified Moment Tensor Analysis and Unified Decomposition of Acoustic Emission Source : Application to In Situ Hydrofracturing Test*, J. of Geophysical Research, 1991, **96**(B4): pp. 6211-6221.